

S-Nitrosylation of AtSABP3 Antagonizes the Expression of Plant Immunity*

Received for publication, September 2, 2008, and in revised form, November 18, 2008. Published, JBC Papers in Press, November 18, 2008, DOI 10.1074/jbc.M806782200

Yi-Qin Wang^{†§1}, Angela Feechan^{‡2}, Byung-Wook Yun[‡], Reza Shafiei^{‡3}, Andreas Hofmann^{¶4}, Paul Taylor[¶], Peng Xue^{||}, Fu-Quan Yang^{||}, Zhen-Sheng Xie^{||}, Jacqueline A. Pallas^{**5}, Cheng-Cai Chu[§], and Gary J. Loake^{†6}

From the [†]Institute of Molecular Plant Sciences and the [¶]Institute of Structural and Molecular Biology, School of Biological Sciences, University of Edinburgh, King's Buildings, Edinburgh EH9 3JR, United Kingdom, the [§]Institute of Genetics and Developmental Biology and the ^{||}Institute of Biophysics, Chinese Academy of Sciences, 15 Datun Road, Andingmenwai, 100101 Beijing, China, and ^{**}Trait Research, Syngenta, Jealott's Hill, Bracknell, Berkshire RG42 6EY, United Kingdom

Changes in cellular redox status are a well established response across phyla following pathogen challenge. In this context, the synthesis of nitric oxide (NO) is a conspicuous feature of plants responding to attempted microbial infection and this redox-based regulator underpins the development of plant immunity. However, the associated molecular mechanism(s) have not been defined. Here we show that NO accretion during the nitrosative burst promotes increasing S-nitrosylation of the *Arabidopsis thaliana* salicylic acid-binding protein 3 (AtSABP3) at cysteine (Cys) 280, suppressing both binding of the immune activator, salicylic acid (SA), and the carbonic anhydrase (CA) activity of this protein. The CA function of AtSABP3 is required for the expression of resistance in the host against attempted pathogen infection. Therefore, inhibition of AtSABP3 CA function by S-nitrosylation could contribute to a negative feedback loop that modulates the plant defense response. Thus, AtSABP3 is one of the first targets for S-nitrosylation in plants for which the biological function of this redox-based post-translational modification has been uncovered. These data provide a molecular connection between the changes in NO levels triggered by attempted pathogen infection and the expression of disease resistance.

Plants have evolved a complex series of integrated defense systems in response to microbial colonization (1, 2). Prominent among these is a repertoire of resistance (R) gene products, which recognize either directly or indirectly pathogen effector proteins, triggering a battery of protective mechanisms (2, 3). A conspicuous feature of this defense response is the synthesis of

nitric oxide (NO),⁷ a key signal for numerous physiological processes in higher eukaryotes (4, 5), which cues the execution of host cells at sites of attempted pathogen infection (6) and drives the expression of a battery of redox-regulated defense genes (7, 8). However, the associated molecular mechanism(s) by which NO orchestrates these diverse cellular responses remains to be determined.

S-Nitrosylation, the addition of a NO moiety to a specific cysteine thiol, to form an S-nitrosothiol (SNO), has emerged as a principal mechanism by which NO orchestrates cellular functions in animals (9). Recently, a number of S-nitrosylated proteins have been identified in *Arabidopsis* (10, 13) and this redox-based post-translational modification shown to regulate the function of a small number of these plant proteins *in vitro* (10–12). However, a potential endogenous role for S-nitrosylation in the regulation of protein function remains to be demonstrated.

Emerging data suggests that SNO turnover may constitute a key mechanism to control cellular SNO levels. The addition of an NO moiety to the antioxidant tripeptide glutathione forms S-nitrosoglutathione (GSNO), which may function as a mobile reservoir of NO bioactivity. An enzyme has recently been uncovered that metabolizes this molecule, governing cellular SNO levels (14). Whereas this GSNO reductase (GSNOR) activity is highly specific for GSNO, it controls the cellular levels of both GSNO and SNO proteins in yeast and mice. Mutations in an *Arabidopsis thaliana* GSNOR (*AtGSNOR1*) impact cellular SNO homeostasis and disable multiple modes of plant disease resistance (15), consistent with a central role for SNOs in the regulation of the plant defense response (16).

Here we show that S-nitrosylation of *A. thaliana* salicylic acid-binding protein 3 (AtSABP3) at cysteine (Cys) 280, during the establishment of plant disease resistance, suppresses both binding of the immune activator, salicylic acid (SA), and the carbonic anhydrase (CA) activity of this protein. Our data suggests that inhibition of AtSABP3 CA function by S-nitrosylation could contribute to a negative feedback loop that modulates the plant defense response. These findings provide a molecular link between the accumulation of NO during

* This work was supported in part by Biological Sciences Research Council Grant BB/D011809/1. The costs of publication of this article were defrayed in part by the payment of page charges. This article must therefore be hereby marked "advertisement" in accordance with 18 U.S.C. Section 1734 solely to indicate this fact.

¹ Recipient of a Royal Society of Edinburgh-NNSC of China joint project.

² Supported by a Biotechnology and Biological Sciences Research Council CASE studentship.

³ Recipient of a Wain Fellowship.

⁴ Present address: Eskitis Institute for Cell and Molecular Therapies, Griffith University, Don Young Road, Brisbane Innovation Park Nathan, Brisbane, Queensland 4111, Australia.

⁵ Present address: Bloomsbury Centre for Bioinformatics, University College London, Gower St., London WC1E 6BT, UK.

⁶ To whom correspondence should be addressed. Tel.: 0131-650-5332; E-mail: gloake@ed.ac.uk.

⁷ The abbreviations used are: NO, nitric oxide; SNO, S-nitrosothiol; AtSABP3, *A. thaliana* SA-binding protein 3; LC/MS-MS, liquid chromatography/mass spectrometry/mass spectrometry; T-DNA, transferred DNA; SA, salicylic acid; CA, carbonic anhydrase; GSNO, S-nitrosoglutathione; GSNOR, S-nitrosoglutathione reductase.

S-Nitrosylation of AtSABP3

attempted pathogen infection and the expression of plant disease resistance.

EXPERIMENTAL PROCEDURES

Detection of Protein S-Nitrosylation—*PstDC3000(avrB)* challenged *Arabidopsis* leaf tissue was frozen in liquid nitrogen at the stated times post-inoculation. Samples were ground to a fine powder under liquid nitrogen and proteins extracted as previously described (10). Protein concentrations were determined according to Bradford (34), with bovine serum albumin as standard. The biotinylation of S-nitrosylated proteins was undertaken essentially as described (17). Biotin-labeled proteins were purified by incubation with streptavidin-agarose and bound proteins eluted with elution buffer (20 mM Hepes, pH 7.7, 100 mM NaCl₂, 1 mM EDTA and 100 mM 2-β mercaptoethanol). Proteins were resolved by SDS-PAGE (35) and the resulting gels stained with either Coomassie Blue or silver staining using a plusone™ kit (GE Healthcare). Protein bands from Coomassie Blue-stained gels were excised and subjected to matrix-assisted laser desorption ionization-time of flight-mass spectrometry analysis. Protein identification was undertaken by searching the National Center for Biotechnology Information nonredundant data base (NCBIInr) using the Mascot search program.

In Vivo and Vitro S-Nitrosylation Assays—Recombinant AtSABP3 was S-Nitrosylated with the stated concentration of the given NO donor in 500-μl volumes for 20 min in darkness. Donors were removed using Micro Bio-Spin P6 columns and the resulting protein was subjected to the biotin switch technique (17). Quantification of endogenous levels of SNO-AtSABP3 during the development of disease resistance was determined as described previously (36). *PstDC3000(avrB)* challenged cells were lysed and subject to immunoprecipitation using an antibody against AtSABP3. Subsequently, the level of SNO formation was determined using the well established 2,3-diaminonaphthalene assay (37), although we found this was not as sensitive as the biotin switch procedure.

Analysis by LC-MS/MS—Liquid chromatography/mass spectrometry/mass spectrometry (LC/MS/MS) experiments were carried out on a Thermo LTQ linear trap instrument equipped with a Thermo microelectrospray source, and a Thermo Surveyor pump and autosample device (Thermo Electron Corporation, San Jose, CA). LC/MS/MS analyses were undertaken by an in-house reverse phase chromatography on an 11-cm fused silica capillary column (100 μm inner diameter) packed with sunchrom 3 μm C18. The peptides were sequentially eluted from the high pressure liquid chromatography column with a gradient of 0 to 100% of buffer B (acetonitrile:water:acetic acid, 80:9.9:0.1) in buffer A (acetonitrile:water:acetic acid, 5:94.9:5.0) at a post-split flow rate of 100 nl/min. The electrospray source parameters were 2.25 KV of electrospray voltage, and 5 V of capillary voltage, the range of *m/z* was from 400 to 2000, normalized collision energy of MS/MS was 35%. The data were analyzed with Bioworks and Qual Browser.

Production of Recombinant AtSABP3 and Antibody Generation—The *AtSABP3* RIKEN cDNA clone pda04430 (*At3g01500*) was cloned into NcoI and XhoI sites of pET32a (Merck Biosciences) and expressed in *Escherichia coli* (BL21).

Recombinant AtSABP3 was affinity purified through nickel-nitrilotriacetic acid-agarose (Merck Biosciences) and used for antibody production.

Site-directed Mutagenesis and Analysis of Protein Structure—Site-directed mutagenesis of AtSABP3 was undertaken using QuikChange® II Site-directed Mutagenesis Kits (Stratagene Corporation). Plasmid pET32a-*AtSABP3* was used as template and primers were designed utilizing the tools from Stratagene and synthesized by Sigma Genosys. The primers were: forward primer: C280S, 5'-TCAATGTGGCCGAAGTGAAAGGGAG-GCGG-3', reverse primer C280S, 5'-CCGCTCCCTT-TCACTTCGGCCACATTGA-3'. Mutations were confirmed by sequencing. The structural model of AtSABP3 was generated using SWISS-MODEL (38) with the structure of pea CA as a template (Protein Data Bank code 1ekj).

SA Binding and CA Activity Assays—Standard SA-binding reactions were carried out as described previously (20). The reaction with 300 nM ¹⁴C-labeled SA (20.5 Ci mmol; 1 Ci = 37 GBq; New England Biolabs) with or without unlabeled SA (10,000-fold molar excess) was carried out in 100 μl of assay buffer (30 mM sodium citrate, pH 6.3, 1 mM EDTA) for 1 h on ice. Unbound ligand was removed with a 1-ml Bio-Spin 6 (Bio-Rad) column by centrifugation for 4 min at 1,000 × *g*. Bound [¹⁴C]SA was quantified by scintillation counting using 50 μl of filtrate. CA enzymatic activity assays of recombinant SABP3 was performed and recorded essentially as reported earlier (39) by using 20 mM Tris-HCl (pH 8.3) as buffer. Chloroplasts were isolated as previously described (20).

Plant Material and Pathogen Inoculations—*Arabidopsis* accession Col-0 and mutants derived from it were grown under 16 h of light at 22 °C and 8 h of darkness at 18 °C. *Arabidopsis* lines possessing a T-DNA insertion into *AtSABP3* were obtained from the Salk T-DNA insertion collection (25), distributed by the Nottingham *Arabidopsis* Stock Center, UK. The *atsabp3-1* line was complemented with a wild-type copy of *AtSABP3* and also transformed with the C260S *AtSABP3* mutant. *PstDC3000* strains were grown, maintained, and utilized as described (40). To monitor bacterial growth *in planta* given *Arabidopsis* lines were inoculated with avirulent *PstDC3000(avrB)* at 10⁵ colony forming units ml⁻¹.

RESULTS

AtSABP3 Is S-Nitrosylated in Vivo and in Vitro—To identify protein targets for S-nitrosylation during the development of plant disease resistance we employed the biotin switch method, a well established technique to monitor SNO formation in animals, which has recently been applied successfully in plants (17). *Pseudomonas syringae* pv. *tomato* (*Pst*) DC3000 expressing the avirulence gene, *avrB* (18), is recognized by the R protein RPM1 (18, 19), triggering the expression of race-specific disease resistance in *Arabidopsis* accession, Col-0. Challenge of this plant line with avirulent *PstDC3000(avrB)* modified the S-nitrosylation status of a series of proteins including *A. thaliana* SA-binding protein 3 (AtSABP3; At3g01500) (20). We had previously established that SNO formation and turnover regulates both the biosynthesis of and signaling by the plant immune activator, SA, impacting multiple modes of plant disease resistance (15). A change in the S-nitrosylation status of

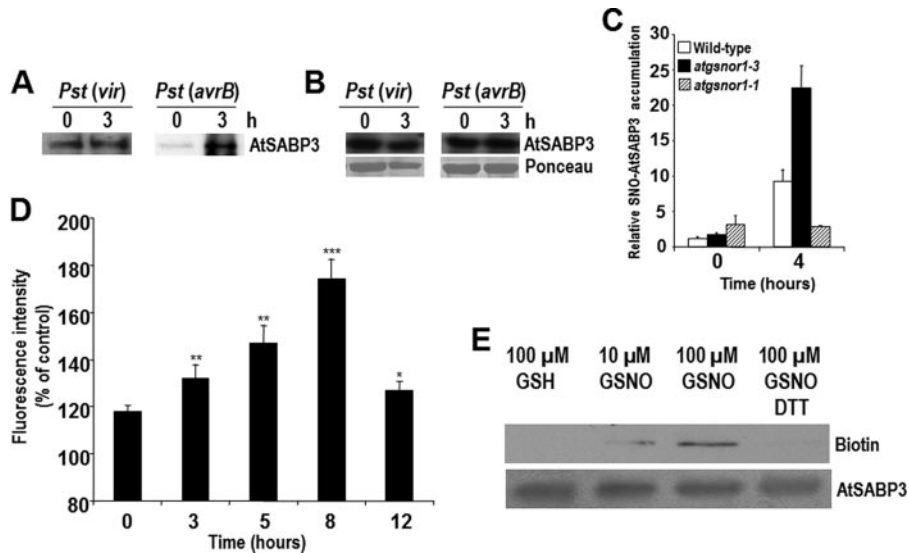


FIGURE 1. AtSABP3 can be S-nitrosylated by NO *in vivo* and *in vitro*. *A*, protein extracts were made from *Arabidopsis* Col-0 leaves infiltrated with 10^7 colony forming units ml^{-1} of either virulent *PstDC3000* or avirulent *PstDC3000(avrB)* at the indicated hours post inoculation. Extracts were subjected to the S-nitrosylation biotin switch assay and subsequently immunoblotted with an antibody raised against AtSABP3. Data shown for *PstDC3000* and *PstDC3000(avrB)* are from independent experiments. *B*, level of AtSABP3 accumulation at 3 h post-inoculation of either virulent *PstDC3000* or avirulent *PstDC3000(avrB)* at 10^7 colony forming units ml^{-1} . Amount of AtSABP3 was determined by immunoblot analysis of corresponding protein extracts in the absence of the biotin switch technique. Ponceau staining is a control for protein loading. *C*, the S-nitrosylation status of AtSABP3 determined in wild-type Col-0, *atgnsnor1-3*, and *atgnsnor1-1* plants. Protein extracts from leaves infiltrated with 10^7 colony forming units ml^{-1} of *PstDC3000(avrB)* at the indicated time points were subjected to the S-nitrosylation biotin switch assay, subsequently immunoblotted with an antibody against AtSABP3 and the resulting blot quantified. Data points show the mean of three samples with error bars representing 95% confidence limits. *D*, leaves of *Arabidopsis* were challenged with *PstDC3000(avrB)* at 10^7 colony forming units ml^{-1} and samples taken at the given h post-inoculation, lysates were immunoprecipitated with an AtSABP3 antibody and the extent of S-nitrosylation quantified using the 2,3-diaminonaphthalene assay. Data are expressed relative to a parallel mock-inoculated control. Data points show the mean of three samples \pm S.D. Student's *t* test confirmed significant differences at: *, $p = 0.05$; **, $p = 0.01$; ***, $p = 0.001$. *E*, S-nitrosylation of recombinant AtSABP3 *in vitro*. Recombinant AtSABP3 was incubated with the stated concentrations of GSNO, GSH, or dithiothreitol (DTT) and subsequently subjected to the S-nitrosylation biotin switch assay. An immunoblot with an antibody against AtSABP3 was employed to check equal protein loading. These experiments were repeated at least twice with similar results.

AtSABP3, a homolog of one of a small number of SA-binding proteins (20–22), therefore, appeared to be of particular significance, although the function of SA binding is unknown. AtSABP3 also exhibits chloroplastic CA activity (20), catalyzing the reversible hydration of CO_2 to HCO_3^- .

To confirm increased S-nitrosylation of AtSABP3 during the defense response, protein extracts from inoculated *Arabidopsis* leaves were subjected to the S-nitrosylation biotin switch procedure and S-nitrosylated proteins purified using streptavidin-agarose. Subsequent Western blot analysis with an antibody raised against AtSABP3 verified enhanced S-nitrosylation of this protein in response to an avirulent but not a virulent strain of *PstDC3000* (Fig. 1A). Congruent immunoblot analysis of AtSABP3 protein levels revealed no significant change in their relative abundance at 3 h post-inoculation with either virulent or avirulent strains of *PstDC3000* (Fig. 1B), suggesting that enhanced SNO-AtSABP3 levels reflected increased S-nitrosylation.

We next determined the extent of SABP3 S-nitrosylation in the *Arabidopsis atgnsnor1-3* and *atgnsnor1-1* mutants, which exhibit either increased or decreased levels of cellular SNOs, respectively (15). SNO-AtSABP3 levels were less conspicuous in *atgnsnor1-1* plants and more pronounced in the *atgnsnor1-3* line relative to wild-type (Fig. 1C), implying that

AtGSNOR1 governs the S-nitrosylation status of AtSABP3 during the defense response. To monitor the profile of SNO-AtSABP3 formation during the establishment of disease resistance, AtSABP3 was immunoprecipitated at various times post *PstDC3000(avrB)* challenge and the extent of S-nitrosylation determined using the 2,3-diaminonaphthalene assay. This analysis suggested that SNO-AtSABP3 formation increased over time during the establishment of disease resistance, peaking at 8 h post-inoculation of *PstDC3000(avrB)* (Fig. 1D). Also, analysis using the 2,3-diaminonaphthalene assay did not appear to be as sensitive for determining the SNO status of AtSABP3 as the biotin switch procedure utilized in Fig. 1C. However, we did not generate the biotin switch data to make a direct comparison.

We also investigated whether S-nitrosylation of AtSABP3 could occur *in vitro*. Recombinant AtSABP3 synthesized in *Escherichia coli* was incubated with a series of GSNO concentrations typically used in tests for *in vitro* S-nitrosylation (10–13) and SNO-AtSABP3 formation was monitored

with the S-nitrosylation biotin switch assay. This analysis revealed that AtSABP3 was S-nitrosylated *in vitro* (Fig. 1E). Furthermore, increasing levels of GSNO promoted SNO-AtSABP3 formation, suggesting S-nitrosylation of AtSABP3 was GSNO concentration dependent. The absence of SNO-AtSABP3 in samples treated with glutathione devoid of NO (GSH) demonstrated the specificity of this post-translational modification. Furthermore, the addition of dithiothreitol strikingly reduced the level of SNO-AtSABP3 formation, which is consistent with the presence of a reversible thiol modification. Collectively, these experiments showed that AtSABP3 was specifically S-nitrosylated *in vitro*.

Identification of Site of AtSABP3 S-Nitrosylation—To identify the target site(s) of S-nitrosylation we carried out LC-MS/MS analysis of GSNO-treated AtSABP3. This tentatively identified Cys²⁸⁰ as the site of S-nitrosylation, however, the intensity of MS/MS spectra obtained was low (data not shown), probably due to the labile nature of SNO formation during sample preparation for this analysis. We therefore carried out LC/MS/MS of S-biotinylated peptides of AtSABP3 following the S-nitrosylation biotin switch assay (Fig. 2, A and B). This approach robustly identified Cys²⁸⁰ as the sole site of S-nitrosylation, confirming our previous LC-MS/MS analysis. Furthermore, Cys²⁸⁰ is embedded within a canonical acid-base

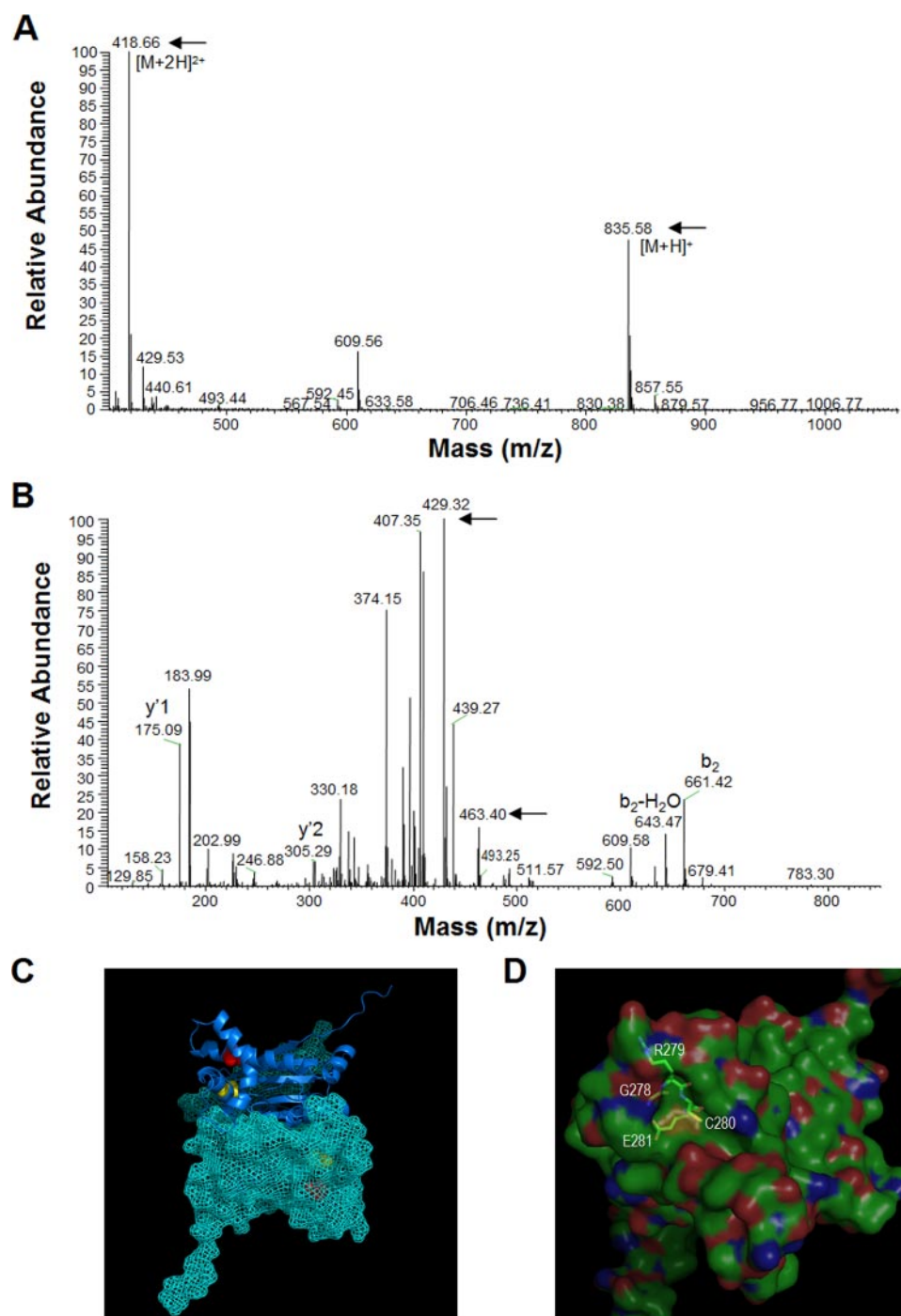


FIGURE 2. The target site for S-nitrosylation of AtSABP3 is identified as Cys²⁸⁰ by mass spectrometry. A, MS/MS spectra of the biotinylated tripeptide C*ER (C*: biotin-HPDP derivatized cysteine, +428), both single (418.66²⁺) and double charged (835.58¹⁺) ions are indicated by arrows. AtSABP3 was treated with 100 μ M GSNO. B, MS/MS spectra of biotinylated tripeptide C*ER. The b₂ (661.42) and b₂-H₂O (643.47) ions indicate a mass shift (+428) was present due to the Cys-N-[6(biotinamido)hexyl]-3'-(2'-pyridyldithio)propionamide (HPDP-biotin) adduct. Two fragment ions, 429.32 and 463.40, indicated by arrows were derived from biotin-HPDP. C, structural model of AtSABP3 shown as a dimeric protein, one monomer is depicted as a ribbon, whereas the other is shown as a surface representation. Cys²⁸⁰ is colored red and Cys²³⁰ is colored yellow in each monomer. The active site zinc (not shown) is coordinated by Cys²³⁰ and the distance of Cys²⁸⁰ to this active site metal ion is 12 Å. D, AtSABP3 structural model revealing that Cys²⁸⁰ is located within a solvent exposed pocket. The structure of a canonical S-nitrosylation motif is superimposed. Yellow indicates the sulfur atom on Cys²⁸⁰. Blue, red, and green colors indicate nitrogen, oxygen, and carbon, respectively.

motif (23), which additionally defines this amino acid as a potential target site for SNO formation. As the three-dimensional structure of a pea CA has been determined (24), we uti-

lized this structure as a template to model the hypothetical three-dimensional conformation of the *Arabidopsis* AtSABP3 (Fig. 2C), to provide us with structural insight into the spatial disposition of Cys²⁸⁰. This residue was present as a solvent-exposed free amino acid at the base of a structural pocket, consistent with it being a target for S-nitrosylation (Fig. 2D).

S-Nitrosylation Impacts AtSABP3 Carbonic Anhydrase Activity—We investigated the potential biological significance of this post-translational modification by assessing its possible impact on the CA activity of AtSABP3. We found that exposure of AtSABP3 to GSNO but not GSH resulted in a dramatic, concentration-dependent decrease in CA activity (Fig. 3A). Furthermore, this inhibition could be reversed by dithiothreitol. Also, an alternative NO donor, S-nitroso-N-acetylpenicillamine, strongly reduced SABP3 CA activity, confirming this effect was NO-dependent (Fig. 3B). Furthermore, this inhibition could be reversed in the presence of dithiothreitol. Together, these results imply that NO through S-nitrosylation of AtSABP3 may function to negatively regulate its CA activity. These findings prompted us to examine chloroplastic CA activity during the defense response. At 8 h post-inoculation of *PstDC3000(avrB)*, the time at which we found AtSABP3 to exhibit maximum S-nitrosylation, CA activity was significantly reduced (Fig. 3C). Thus, chloroplastic CA activity is modulated during the establishment of plant disease resistance. Next we determined this activity in *atgsnor1-1* and *atgsnor1-3* plants (15). The reduction of CA activity was decreased in *atgsnor1-1* plants but increased in the *atgsnor1-3* mutant line (Fig. 3C). Collectively, our findings provide a direct molecular link between S-nitrosylation of AtSABP3 and CA activity. However, it is possible that other mechanisms

may also contribute to the regulation of AtSABP3 activity.

To investigate the potential role of Cys²⁸⁰ in AtSABP3 function, we carried out site-directed mutagenesis to replace this

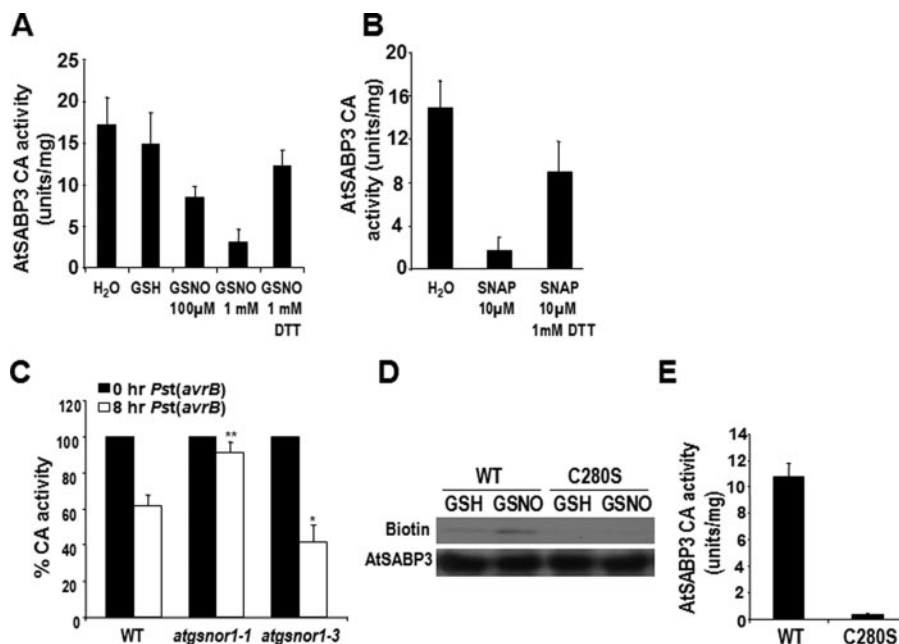


FIGURE 3. The CA activity of AtSABP3 is negatively regulated by S-nitrosylation of Cys²⁸⁰. *A*, recombinant AtSABP3 was incubated with the given concentrations of GSNO, GSH, and dithiothreitol (DTT) and the CA activity of this protein determined. *B*, the CA activity of recombinant AtSABP3 was determined following exposure to the NO donor S-nitroso-N-acetylpenicillamine (SNAP). *C*, relative chloroplastic CA activity measured in the stated plant genotypes at 8 h post-inoculation of *PstDC3000(avrB)*. Data points show the mean \pm S.D. of three samples. Student's *t* test confirmed significant differences. *, $p = 0.02$; **, $p = 0.01$. *D*, recombinant wild-type (WT) AtSABP3 and the C280S mutant derivative were incubated with either 100 μ M GSNO or GSH and subsequently these proteins were subjected to the S-nitrosylation biotin switch technique and subsequently immunoblotted with an antibody against biotin. Equal protein loading of individual samples was determined by immunoblotting with an antibody against AtSABP3. *E*, the CA activity of recombinant wild-type AtSABP3 and the C280S mutant derivative were determined as described above. For *A*, *B*, and *E*, error bars represent 95% confidence limits. These experiments were repeated at least twice with similar results.

residue with serine (Ser) and subsequently synthesized the corresponding recombinant protein in *E. coli*. As expected, C280S AtSABP3 could not be S-nitrosylated (Fig. 3D), further confirming Cys²⁸⁰ as the site of S-nitrosylation. We then assessed the CA activity associated with this AtSABP derivative. The C280S mutant was found to be strikingly reduced in CA activity (Fig. 3E). This was unexpected because this residue is some distance from the active site and previous structure-function studies of this enzyme have not uncovered a significant role for Cys²⁸⁰ in CA activity (24). Nevertheless, our data imply that structural changes at this position may compromise CA activity, consistent with our findings that S-nitrosylation at Cys²⁸⁰ negatively regulates the CA activity of AtSABP3.

Role of AtSABP3 in Disease Resistance—AtSABP3 has previously been shown to bind SA with high affinity (20). However, amino acid residues required for SA binding have not yet been identified and the binding of this small molecule does not affect CA activity, suggesting these functions are independent (20). We next explored if S-nitrosylation of Cys²⁸⁰ could also modulate the SA binding activity of AtSABP3. This activity was assessed in the presence of [¹⁴C]SA with or without excess unlabeled SA. To monitor the impact of S-nitrosylation, AtSABP3 was incubated with 1 mM GSNO prior to the determination of [¹⁴C]SA binding (Fig. 4A). Our results suggested that S-nitrosylation of AtSABP3 significantly decreased SA binding. We also investigated the binding of this small molecule in the C280S AtSABP3 mutant. In the absence of GSNO exposure,

this mutant derivative bound a similar amount of [¹⁴C]SA to wild-type AtSABP3, revealing that C280S AtSABP3 retains full SA binding capacity (Fig. 4B). Furthermore, exposure of C280S AtSABP3 to GSNO did not impact [¹⁴C]SA binding. Collectively, these data imply that S-nitrosylation of Cys²⁸⁰ AtSABP3 reduces SA binding. Thus, increasing S-nitrosylation of AtSABP3 during the defense response may reduce both the SA binding ability and CA activity of AtSABP3.

To determine a possible role for AtSABP3 in the establishment of disease resistance in *Arabidopsis*, we identified two independent *atsabp3* loss-of-function alleles from the Salk Institute transferred DNA (T-DNA) insertion collection (25). The *atsabp3-1* and *atsabp3-2* T-DNA lines were challenged with *PstDC3000(avrB)* and pathogen growth monitored over time. Both *atsabp3* alleles supported more *PstDC3000(avrB)* growth compared with wild-type (Fig. 4C). Thus, AtSABP3 is required for a full defense response against this bacter-

ial strain. To assess whether CA activity is required for AtSABP3-dependent disease resistance, we utilized an *atsabp3-2 Arabidopsis* line containing either a wild-type AtSABP3 transgene or the C280S AtSABP3 mutant derivative. No increased susceptibility to *PstDC3000(avrB)* was observed in the *atsabp3-2 Arabidopsis* line containing the wild-type AtSABP3 transgene (Fig. 4D). In contrast, *PstDC3000(avrB)* growth was increased in *atsabp3-2* plants possessing the mutant C280S AtSABP3 derivative relative to wild-type. Taken together, these data suggest that the CA activity of AtSABP3 contributes to resistance against *PstDC3000(avrB)*.

DISCUSSION

The engagement of a nitrosative burst in response to attempted pathogen infection is a prominent feature of the plant defense response (6, 7, 26). Although NO has long been thought to have central signaling functions in the establishment of plant disease resistance (6, 7) the molecular machinery underpinning these responses has remained largely enigmatic. In the present study, we have identified AtSABP3 as a target for S-nitrosylation during the expression of disease resistance. This post-translational modification curbs the CA activity of AtSABP3, which is required for disease resistance, potentially contributing to a negative feedback loop that modulates the defense response. Thus, whereas carefully regulated S-nitrosylation of AtSABP3 may be integral to control the expression of disease resistance, the sustained absence of AtSABP3 func-

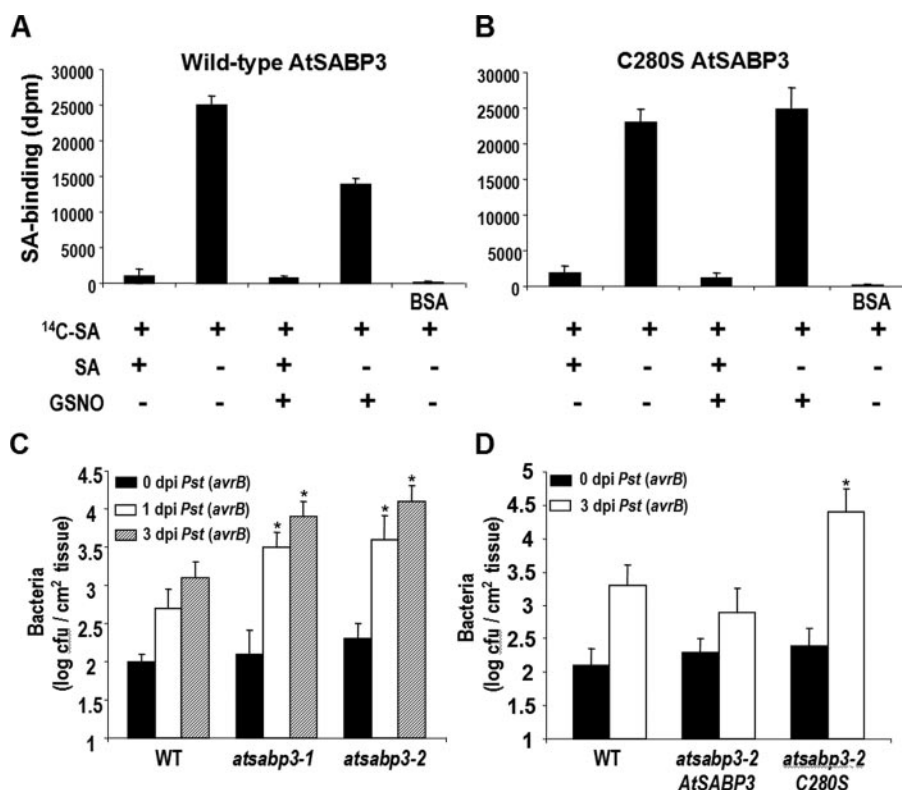


FIGURE 4. S-Nitrosylation of AtSABP3 blunts SA binding and the CA activity of AtSABP3 is required for disease resistance. *A*, the affinity of wild-type AtSABP3 for SA was determined using 300 nM ¹⁴C-labeled SA (20.5 Ci mmol; 1 Ci = 37 GBq) in the presence or absence of unlabeled SA (10,000-fold molar excess) or 100 μM GSNO. Following removal of unbound ligand, bound [¹⁴C]SA was quantified by scintillation counting. *B*, the affinity of the C280S AtSABP3 mutant for ¹⁴C-labeled SA in the presence or absence of excess unlabeled SA and 100 μM GSNO was undertaken as described above. For *A* and *B*, data points show the mean of three samples with error bars representing 95% confidence limits. *C*, growth of *PstDC3000(avrB)* in the given plant lines at the indicated days post inoculation. *D*, growth of *PstDC3000(avrB)* in the stated plant lines at the shown dpi. For *C* and *D*, data points show the mean ± S.D. of three samples. Student's *t* test confirmed significant differences. *, *p* = 0.01. These experiments were repeated at least twice with similar results.

tion appears to lead to enhanced pathogen susceptibility. In this report, we have only monitored the SNO status of AtSABP3 in response to virulent *PstDC3000* at an early time point post-inoculation. It is conceivable that at later stages of infection this pathogen might promote increased SNO-AtSABP3 formation as a mechanism to aid pathogenesis.

The emerging data is highlighting a key function for SABP3 and its homologs in disease resistance. In this context, tobacco SABP3 has previously been shown to be required for *R* gene-dependent defense responses (20). Moreover, a potato homolog of this gene was found to be quickly suppressed during the development of late blight disease and silencing *SABP3* in *Nicotiana benthamiana* resulted in increased pathogen growth (27). Our data, in addition to these findings, supports a role for CA activity in disease resistance. CA enzymes are evolutionary conserved across phyla and are thought to play a key role in lipolysis (28). In multiple plant species, CA function is required for lipid biosynthesis within the chloroplast, possibly due to its interaction with acetyl-CoA carboxylase and the enzymes of the fatty acid synthase complex, where it may efficiently “channel” carbon into fatty acid (28). This role for the CA activity of *AtSABP3* may be particularly pertinent within the context of the plant defense response because lipid-based signals are thought to be fundamental to the development of disease resistance (29, 30).

Collectively, our findings suggest that increasing *S*-nitrosylation of AtSABP3 during the progression of the nitrosative burst may blunt its cognate CA activity, reducing fatty acid biosynthesis in the chloroplast and thereby diminishing the transient production of lipid-based defense cues. Formation of SNO-AtSABP3 might therefore govern a negative feedback loop that serves to dampen defense signaling. Consistent with this hypothesis, *atgsnor1-3* plants exhibit increased levels of SNO-AtSABP3, decreased CA activity, diminished and delayed defense responses, and are compromised in resistance against *PstDC3000(avrB)* (15). In contrast, *atgsnor1-1* plants show decreased levels of SNO-AtSABP3, increased CA activity, accelerated defense responses, and display resistance against ordinarily virulent pathogens (15). The prompt engagement of a negative feedback loop, reported here, parallels recent findings in the signaling network that underpins perception of the lipid-based defense signal, jasmonate-isoleucine (31).

Although the exogenous addition of numerous pharmacological agents has suggested NO regulates a wide variety of responses (5–7) the *in planta* molecular detail underpinning these processes remains to be established. *S*-Nitrosylation has emerged as a principal mechanism by which NO exerts biological effects in animal systems, with a large variety of proteins reported as targets for this key post-translational modification (9, 23). By demonstrating that SNO-AtSABP3 formation governs the engagement of a negative feedback loop during the defense response, we provide molecular characterization of a possible *in vivo* function for *S*-nitrosylation, suggesting this process may also represent a fundamental regulatory process in plants. Furthermore, recent findings imply that *S*-nitrosylation of NPR1, a key transcriptional regulator of defense gene expression, promotes the oligomerization of this protein, preventing its translocation to the nucleus, which consequently suppresses the development of plant immunity (32). Also, *S*-nitrosylation of peroxiredoxin II E has lately been proposed to promote the accretion of peroxy-nitrite leading to increased tyrosine nitration, which might help drive the programmed execution of directly challenged plant cells, a routine feature of *R* gene-mediated disease resistance (11). Thus, SNO formation may target multiple nodes of the plant defense signaling network resulting in a variety of regulatory permutations that collectively optimize cellular responses. This is reminiscent of the NF-κB immune signaling network in animals, where

the activity of manifold components is controlled by S-nitrosylation (9, 33).

Acknowledgments—We thank Roger Innes (Indiana University, Bloomington) for PstDC3000(avrB). *Arabidopsis* T-DNA insertion mutants were obtained from the SIGNAL collection. We also thank Xinnian Dong, Yasuomi Tada, and Steven Spoel for helpful discussions.

REFERENCES

- Chisholm, S. T., Coaker, G., Day, B., and Staskawicz, B. J. (2006) *Cell* **124**, 803–814
- Dangl, J. L., and Jones, J. D. (2001) *Nature* **411**, 826–833
- Staskawicz, B. J., Mudgett, M. B., Dang, J. L., and Galan, J. E. (2001) *Science* **292**, 2285–2289
- Ingarro, L. J. (2000) *Nitric Oxide Biology and Pathobiology*, Academic Press, San Diego, CA
- Lamattina, L., Garcia-Mata, C., Graziano, M., and Pagnussat, G. (2003) *Annu. Rev. Plant Biol.* **54**, 109–136
- Delledonne, M., Xia, Y., Dixon, R. A., and Lamb, C. (1998) *Nature* **394**, 585–588
- Durner, J., Wendehenne, D., and Klessig, D. F. (1998) *Proc. Natl. Acad. Sci. U. S. A.* **95**, 10328–10333
- Polverari, A., Molesini, B., Pezzotti, M., Buonauro, R., Marte, M., and Delledonne, M. (2003) *Mol. Plant Microbe Interact.* **16**, 1094–1105
- Hess, D. T., Matsumoto, A., Kim, S.-O., Marshall, H. E., and Stamler, J. S. (2005) *Nat. Rev. Mol. Cell Biol.* **6**, 150–166
- Lindermayr, C., Saalbach, G., and Durner, J. (2005) *Plant Physiol.* **137**, 921–930
- Romero-Puertas, M. C., Campostrini, N., Matte, A., Righetti, P. G., Perazzolli, M., Zolla, L., Roepstorff, P., and Delledonne, M. (2007) *Plant Cell* **19**, 4120–4130
- Lindermayr, C., Saalbach, G., Bahnweg, G., and Durner, J. (2006) *J. Biol. Chem.* **281**, 4285–4291
- Belenghi, B., Romero-Puertas, M. C., Vercammen, D., Brackener, A., Inzé, D., Delledonne, M., and Van Breusegem, F. (2007) *J. Biol. Chem.* **282**, 1352–1358
- Liu, L., Hausladen, A., Zeng, M., Que, L., Heitman, J., and Stamler, J. S. (2001) *Nature* **410**, 490–494
- Feechan, A., Kwon, E., Yun, B.-W., Wang, Y., Pallas, J. A., and Loake, G. J. (2005) *Proc. Natl. Acad. Sci. U. S. A.* **102**, 8054–8059
- Wang, Y., Yun, B.-W., Kwon, E., Hong, J.-K., Yoon, J., and Loake, G. J. (2006) *J. Exp. Bot.* **57**, 1777–1784
- Jaffrey, S. R., Erdjument-Bromage, H., Ferris, C. D., Tempst, P., and Snyder, S. H. (2001) *Nat. Cell Biol.* **3**, 193–197
- Bisgrove, S. R., Simonich, M. T., Smith, N. M., Sattler, A., and Innes, R. W. (1994) *Plant Cell* **6**, 927–933
- Grant M. R., Godiard, L., Straube, E., Ashfield, T., Lewald, J., Sattler, A., Innes, R. W., and Dangl, J. L. (1995) *Science* **269**, 843–846
- Slaymaker, D. H., Navarre, D. A., Clark, D., del Pozo, O., Martin, G. B., and Klessig, D. F. (2002) *Proc. Natl. Acad. Sci. U. S. A.* **99**, 11640–11645
- Chen, Z., Silva, H., and Klessig, D. F. (1993) *Science* **262**, 1883–1886
- Kumar, D., and Klessig, D. F. (2003) *Proc. Natl. Acad. Sci. U. S. A.* **100**, 16101–16106
- Hess, D. T., Matsumoto, A., Nudelman, R., and Stamler, J. S. (2001) *Nat. Cell Biol.* **3**, E1–E3
- Kimber, M. S., and Pai, E. F. (2000) *EMBO J.* **19**, 1407–1418
- Alonso, J. M., Stepanova, A. N., Leisse, T. J., Kim, C. J., Chen, H. M., Shinn, P., Stevenson, D. K., Zimmerman, J., Barajas, P., Cheuk, R., Gadriab, C., Heller, C., Jeske, A., Koesema, E., Meyers, C. C., Parker, H., Prednis, L., Ansari, Y., Choy, N., Deen, H., Geralt, M., Hazari, N., Hom, E., Karnes, M., Mulholland, C., Ndubaku, R., Schmidt, I., Guzman, P., Aguilar-Henonin, L., Schmid, M., Weigel, D., Carter, D. E., Marchand, T., Risseeuw, E., Brogden, D., Zeko, A., Crosby, W. L., Berry, C. C., and Ecker, J. R. (2003) *Science* **301**, 653–656
- Hong, J.-K., Yun, B.-W., Kang, J.-G., Raja, M. U., Kwon, E.-J., Sorhagen, S., Chu, C., Wang, Y.-Q., and Loake, G. J. (2008) *J. Exp. Bot.* **59**, 147–154
- Restrepo, S., Myers, K. L., del Pozo, O., Martin, G. B., Hart, A. L., Buell, C. R., Fry, W. E., and Smart, C. D. (2005) *Mol. Plant Microbe Interact.* **18**, 913–922
- Hoang, C. V., and Chapman, K. D. (2002) *Plant Physiol.* **128**, 1417–1427
- Chandra-Shekar, A. C., Venugopal, S. C., Barman, S. R., Kachroo, A., and Kachroo, P. (2007) *Proc. Natl. Acad. Sci. U. S. A.* **104**, 7277–7282
- Nandi, A., and Shah, J. (2004) *Plant Cell* **16**, 465–477
- Chini, A., Fonseca, S., Fernández, G., Adie, B., Chico, J. M., Lorenzo, O., Garcia-Casado, G., López-Vidriero, I., Lozano, F. M., Ponce, M. R., Micol, J. L., and Solano, R. (2007) *Nature* **448**, 666–671
- Yasuomi, T., Spoel, S. H., Pajerowska-Mukhtar, K., Mou, Z., Song, J., Wang, C., Zuo, J., and Dong, X. (2008) *Science* **321**, 952–956
- Marshall, H. E., Hess, D. T., and Stamler, J. S. (2004) *Proc. Natl. Acad. Sci. U. S. A.* **101**, 8841–8842
- Bradford, M. M. (1976) *Anal. Biochem.* **77**, 248–254
- Laemmli, U. K. (1970) *Nature* **227**, 680–685
- Haendeler, J., Hoffmann, J., Tischler, V., Berk, B. C., Zeiher, A. M., and Dimmeler, S. (2002) *Nat. Cell Biol.* **4**, 743–749
- Miles, A. M., Chen, Y., Owens, M. W., and Grisham, M. B. (1995) *Methods (Amst.)* **7**, 40–45
- Guex, N., and Peitsch, M. C. (1997) *Electrophoresis* **18**, 2714–2723
- Wilbur, K. M., and Anderson, N. G. (1948) *J. Biol. Chem.* **176**, 147–154
- Whalen, M. C., Innes, R. W., Bent, A. F., and Staskawicz, B. J. (1991) *Plant Cell* **3**, 49–59